Resistance of a commercial magnetorheological fluid to penetration

To cite this article: K F Plunkett *et al* 2013 *J. Phys.: Conf. Ser.* **412** 012023

View the article online for updates and enhancements.

Resistance of a commercial magnetorheological fluid to penetration

K F Plunkett[1], MA Imam[2], B Rath[2] and H Conrad[1]

[1] Materials Science and Engineering Dept., North Carolina State University, Raleigh, NC 27695-7907, USA

[2] Materials Science and Component Technology Directorate, Naval Research Laboratory, Washington, D.C. 20375, USA

E-mail: kenfplunkett@gmail.com

Abstract. The stress, σ, required to penetrate a commercial magnetorheological (MR) fluid exposed to an applied magnetic field, B, in the range of 0 - 0.25 Tesla was determined for: (a) a constant, continuous field and (b) on-off field. With constant field application, it was found that σ vs. the penetration depth, x, of the cylindrical indenter into the MR fluid at a constant rate of 0.12-0.18 mm/s was parabolic in form, namely $\sigma = \sigma_o x^n$ where $\sigma_0 = AH$, A = 1.7 kPa/(kA/m) and n = 0.3-0.5. The magnitude of σ_o is approximately six times that of the shear yield stress, τ_y, of the MR fluid. A model is proposed to explain the resistance to penetration into the MR fluid with the constant field. The results obtained in the on-off field tests and the in-out tests are in keeping with the model.

1. Introduction

A new class of materials of interest is magnetorheological (MR) fluids for wide range of applications. These fluids consist of micron-sized ferromagnetic particles suspended in a dielectric liquid such as a hydrocarbon oil or silicone oil [1]. With application of a magnetic field the viscosity of the suspension changes in times of the order of milliseconds [2] from Newtonian behavior to Bingham behavior with a so-called yield stress. The shear yield stress, τ_y, is the stress required to rupture the chain-like arrangement of the particles aligned along the magnetic flux [3]. The shear yield stress of typical MR fluids ranges from 10 to 60 kPa for a magnetic field H_{MRF} = 100 kA/m [1].

Theoretical considerations by Ginder and Davis [4] give for the yield stress prior to magnetic saturation of the particles in an MR fluid:

$$\tau_y = K_1 H_{MRF}^{\alpha} \tag{1}$$

and upon saturation

$$\tau_y = K_2 M_S^{\alpha} \tag{2}$$

where K_1 and K_2 are functions of the volume fraction φ of the particles, H_{MRF} is the magnetic field within the suspension, α is a constant on the order of 1-2 and M_s is the magnetic saturation of the particles. Tang and Conrad [5] found reasonable agreement between experiment and theory for shear tests on a suspension of carbonyl iron in silicone oil.

Carlsen [1] proposed the following empirical expression for the yield stress of MR fluids

$$\tau_y = (2.72 \times 10^5 \varphi^{1.534} C)\tanh(6.33 \times 10^{-6} H_{MRF}) \tag{3}$$

where the constant C ≈ 1 and H_{MRF} is given by

$$B = 1.91\varphi^{1.311}[1 - \exp(-10.97\mu_0 H_{MRF})] + \mu_0 H_{MRF} \tag{4}$$

B is the applied magnetic field in Tesla and μ_0 the vacuum permeability.

To the authors' knowledge, no prior study on the strength of MR fluids has been performed in which penetration techniques have been implemented in the presence of an applied field. The objective of the present investigation was to determine their behavior in a compression (squeeze) mode.

2. Experimental

2.1. MR Fluid
The MR fluid employed in the present tests was Lord MRF-132DG, which was provided gratis by the Lord Corporation, Cary, North Carolina. The specifications pertaining to this fluid can be found in the Lord Technical Data sheets, located on the company's website. These give that the fluid consists of ~0.30 volume fraction (φ) magnetic particles (presumably carbonyl iron) suspended in a hydrocarbon oil and has a yield stress in shear of 55 kPa at H_{MRF} = 150 kA/m. Typical magnetic properties of the fluid are given in Figure 1.
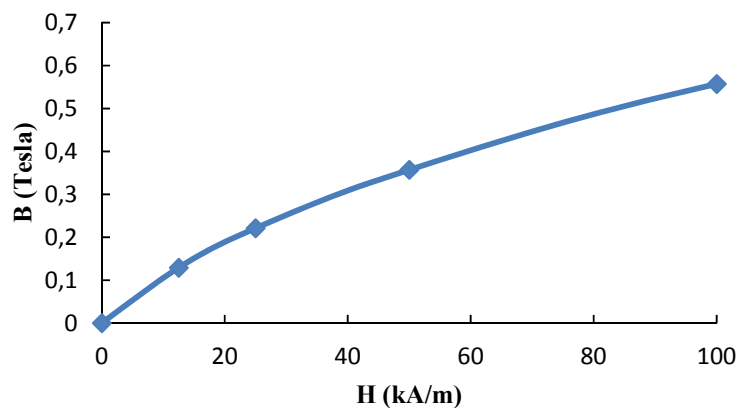

Figure 1. B vs. H_{MRF} given by Lord Corp. for their MRF-132DG.

2.2. Magnetic field apparatus
A schematic of the apparatus developed by us to apply the magnetic field during a compression test and the geometry and dimensions of the container and indenter are presented in Figure 2. The DC power supply consisted of two HP 6032A (60 V, 50 A) units provided by the U.S. Naval Research Laboratory and connected in series. The magnetic field in the air gap between the poles was measured with a F.W.

Bell IDR-329-T-UL: DC Kilogauss meter with an ultrathin transverse probe. A plot of the measured magnetic field in the airgap of 22 mm (outer diameter of the Al MR fluid container) between the curved pole pieces vs. the electric current, I, in the electromagnetic coil is presented in Figure 3. The flux is roughly proportional to the current up to 2 A, after which it increases at a decreasing rate.
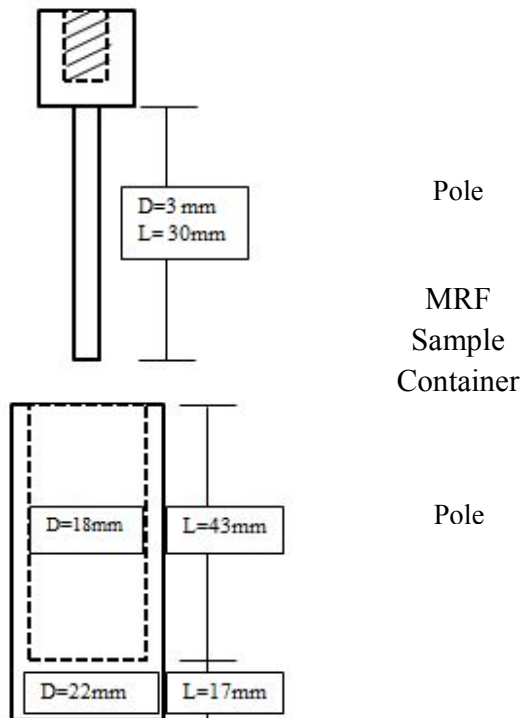

Figure 2. Schematic of the manner in which the magnetic field was applied to the MR fluid. Note the iron core poles were machined to fit around the Al MRF container. Also shown are the geometry and dimensions of the MR fluid container and the indenter. For testing, the indenter was located directly above the center of the sample container and was vertically lowered into the MRF.
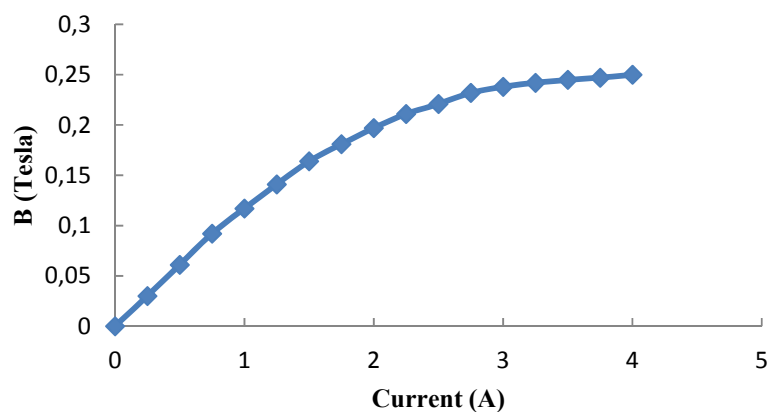

Figure 3. Measured magnetic flux in the 22 mm airgap (outer diameter of the Al MR fluid container) vs. the current in the electromagnetic coil.

Figure 4. Photograph of the setup by which the compression tests were performed.

2.3. Compression (Penetration) tests

A photograph of the set-up by which the compression tests were performed is shown in Figure 4. The compressive load was applied at a fixed displacement rate of 0.12 to 0.15 mm/s by a commercial RSL Digital Displacement Loading Frame tension-compression mechanical test machine. Particular displacement rates are displayed on a per figure basis if applicable. The load was measured and recorded using a Futek LRM 200, 1 lb, JR S-Beam load cell.

Four types of compression (indentation) tests were performed:

- Tests with a fixed magnetic field throughout the entire test (Type A).
- On-off tests in which the field is alternately turned on and off during the test (Type B).
- In-out tests in which the indenter is applied with a fixed magnetic field, then retracted while the field is still maintained (Type C).
- Tests in which Type B was performed during a Type C test (Type D).

The Type A tests provide a measure of the resistance of the MR fluid to penetration; the Type B provides information on how quickly the resistance decreases following the removal of the field; the Type C provides information on the frictional or surface energy resistance imposed on the penetrator by contact of its cylindrical surface with the MR fluid, and Type D provides information on the effect of on-off cycles on the friction resistance. The resistance to penetration in each test is here reported as a nominal compression (or tensile) stress given by $\sigma = P/A$, where P is the load and A is the cross sectional area of the penetrating end of the indenter.

The following procedure was employed in performing a test with a constant field:

- The MR fluid was vigorously shaken and poured into the Al container.
- The indenter was centered and then lowered to within 0.5 to 1 mm above the surface of the MR fluid.
- The power supply was turned on to provide the magnetic field.
- The mechanical test machine was activated and the load vs. displacement was recorded.
- The test was terminated following a penetration of ~ 20 mm, and the penetrator withdrawn.

Similar procedures were employed in the on-off and in-out tests.

3. Results

3.1. Continuous magnetic field

Plots of the compressive stress vs. the displacement of the indenter as a function of the current passing through the electromagnetic coil are presented in Figure 5. The σ vs. displacement curves are parabolic in form. Incremental measurements using the gauss meter indicated a homogeneous field within the empty sample container. Field homogeneity could not be directly verified in situ due to the gauss meter's fragility, but it is inferred to be so. The aberrations in Figure 5's parabolic curves are the result of environmental vibrations being detected by the load cell. Converting the current to applied magnetic field, B, (Figure 3) the stress required for a displacement of 1, 5, 10, and 15 mm vs. B is given by Figure 6. It should be noted that for each displacement, x, the curvature of the plot is initially hyperbolic to B = 0.06 Tesla and then becomes essentially linear to B = 0.25 Tesla, the largest field attainable with our electromagnet setup. There is however some indication that for x = 20 mm, the stress becomes constant for B > 0.24 Tesla. Further work is required to determine whether this is in fact the case.

It should also be noted that during a compression test a brown translucent liquid, presumably the host hydrocarbon oil with no visible evidence of the magnetic particles, was squeezed up between the outer surface of the indenter and magnetized MR fluid. Moreover, the compressive stresses in the present tests are between 1 and 2 orders of magnitude larger than those normally obtained for the shear of MR fluids [1, 4, 5].
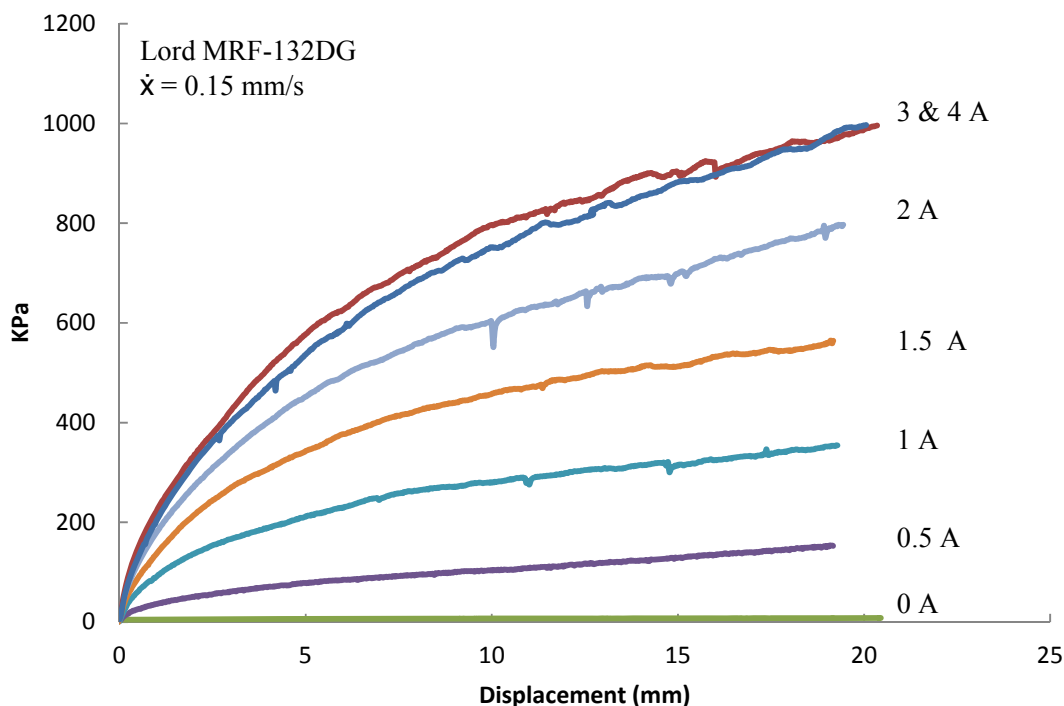

Figure 5. Compressive stress vs. displacement as a function of the current in the electromagnet in increments of 0.5 A. Stress curves for 3 and 4 A are provided to indicate the magnetic saturation of the electromagnet.
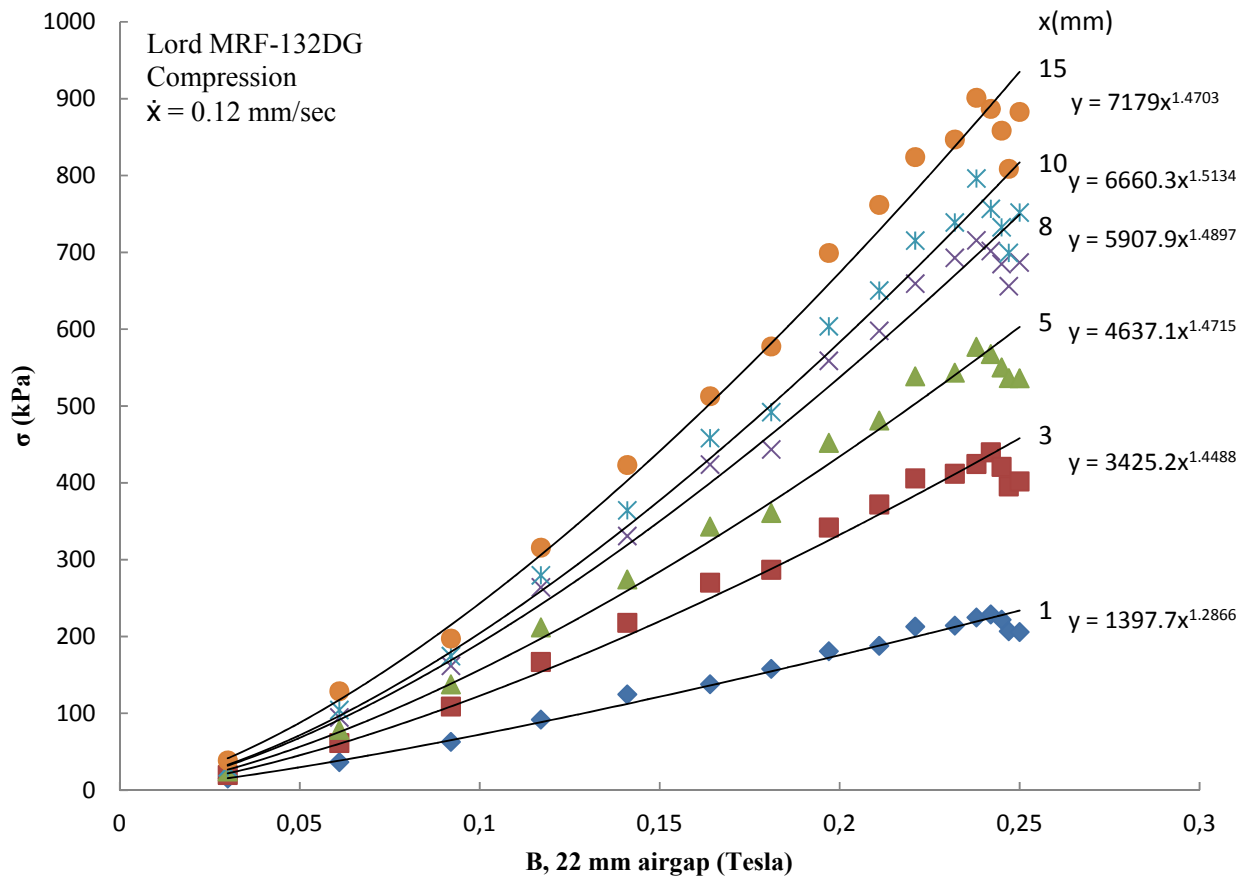
Figure 6. σ vs. B as a function of displacement, x; From the bottom, displacements are recorded at 1, 3, 5, 8, 10, and 15 mm. Equations for 1, 3, and   15 mm lines are y = 1397.7x$^{1.2866}$, y = 3425.2x$^{1.4488}$, and y = 7179x$^{1.4703}$ respectively.

3.2. On-off tests
The stress-displacement curves obtained in the tests in which the power supply to the electromagnet was periodically turned on and off are presented in Figure 7 for a current of 2 A. Analogous results were obtained for using a current of 1 A and 3 A. Included are the results for 2 cycles and 10 cycles. Also included in the figure is the σ vs. displacement curve obtained in the constant continuous field tests. To be noted in Figure 7 is: (a) the decrease in load when the field is turned off is abrupt and less than the response time of the recorder (< 0.25 seconds), (b) upon turning the field on, the initial increase in stress is abrupt up to a "yield stress" (σ_y) and then increased at a less rapid rate, (c) σ_y decreased the more frequent the number of on-off cycles, (d) the ratio σ_y/σ became smaller the greater the number of on-off cycles and the higher the applied magnetic field.
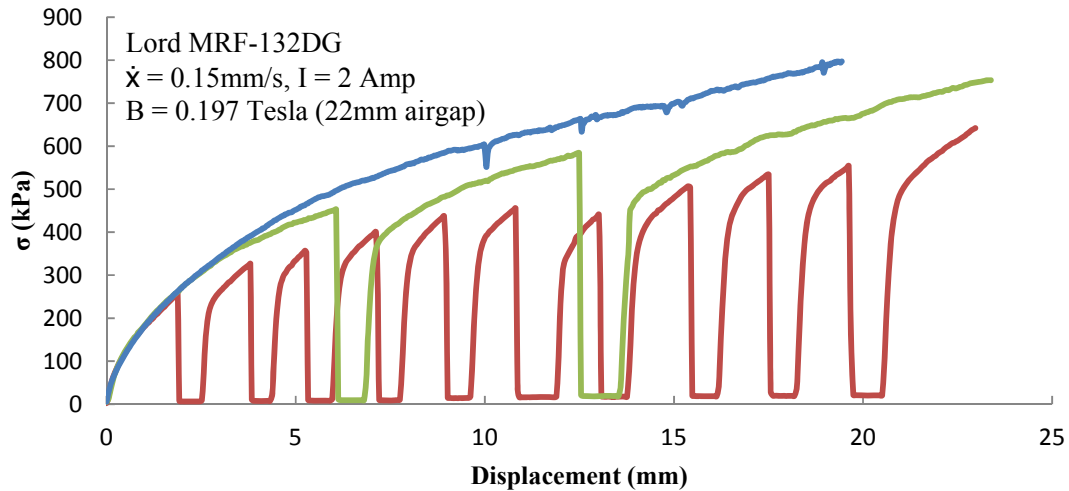
Figure 7. On-off field cycling tests (2 and 10 cycles) with electromagnet current, I = 2A, compared to the behavior for a continuous current of 2 A.

3.3. In-out tests

The behavior in the tests in which the indenter first penetrated the MR fluid with the field on, and then was retracted from the fluid, with the same field strength and displacement rate, is shown in Figure 8 for the field corresponding to 2A. To be noted is that immediately following the direction change of the indenter, the MR fluid exerts a resistive, pulling, force on the indenter, the magnitude of which is ~1/4 of the compressive force prior to retraction. This force is interpreted to result from shear friction on the indenter's walls. The negative pressure is similar when the field is turned on and off as well as when the field was held constant throughout the test. Also to be noted is that the tensile force decreases as the indenter is retracted from the MR fluid. Further, the decrease in tensile force which occurs when the field is turned off during the extraction becomes less with the extraction.
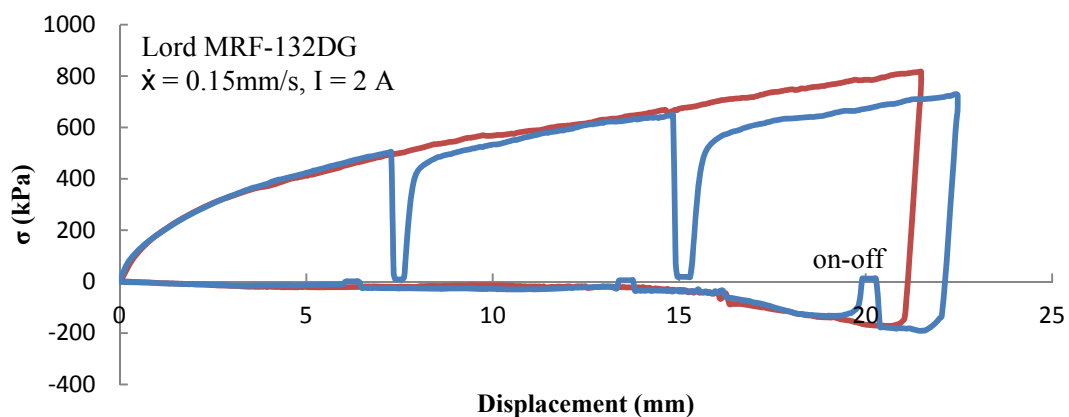

Figure 8. In-out tests with the on-off cycling test superimposed on a continuous test with an electromagnet current of I = 2 A.

4. Discussion

The parabolic nature of the σ vs. displacement curves in Figure 5 represent equations of the form $\sigma = \sigma_0 x^n$, which equate to

$$log\ \sigma = log\ \sigma_0 + n \log\ x \tag{5}$$

where σ_0 is the compressive stress for x = 1 mm and n is the slope of the plot of log σ vs. log x. Log-log plots of the σ vs. displacement curves for several continuous electromagnetic currents are presented in Figure 9. The currents have here been converted to applied magnetic field, B, according to Figure 3. The results in Figure 9 are reasonably fit by straight lines with σ_0 increasing with magnetic field strength and n ≈ 0.3-0.5 increasing with field strength. A plot of σ_0 vs. H_{MRF} taken from Fig.3 is shown in Figure 10. There occurs a reasonable fit to a straight line with a slope of 12.3 (kPa)/(kA/m). This slope is ~ 6 times that given in the Lord Technical Data sheet for the shear stress, $\tau_{y,}$ in the same H_{MRF} range and is included in Figure 15. The linear fit for σ_0 vs H_{MRF} is in accord with theoretical considerations of τ_y [4,5], and the magnitude of σ_o is effectively six times larger.
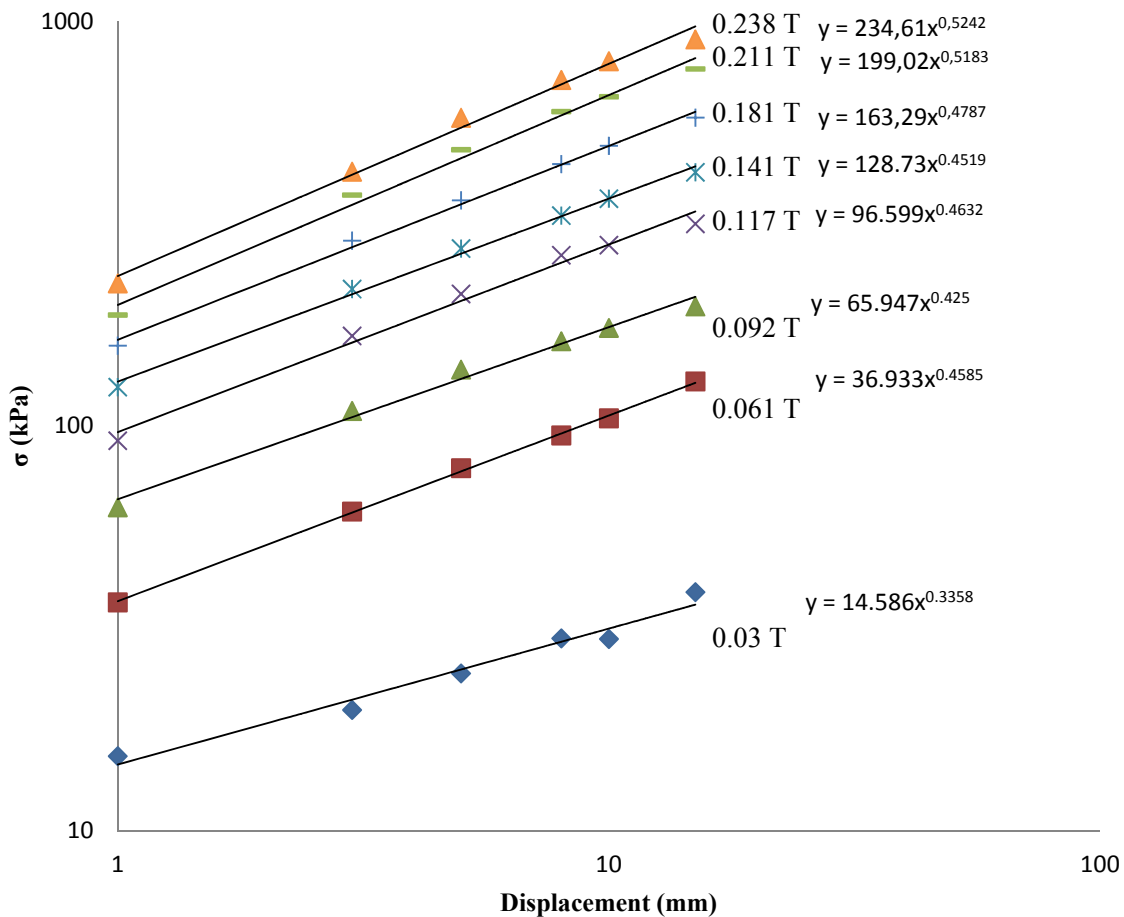

Figure 9. Log-log plots of the σ vs. displacement curves for a constant field as a function of the applied field, B, (Tesla); Field strengths for equation denoted lines are .03 T, .061 T, and .238 T, from the bottom respectively.
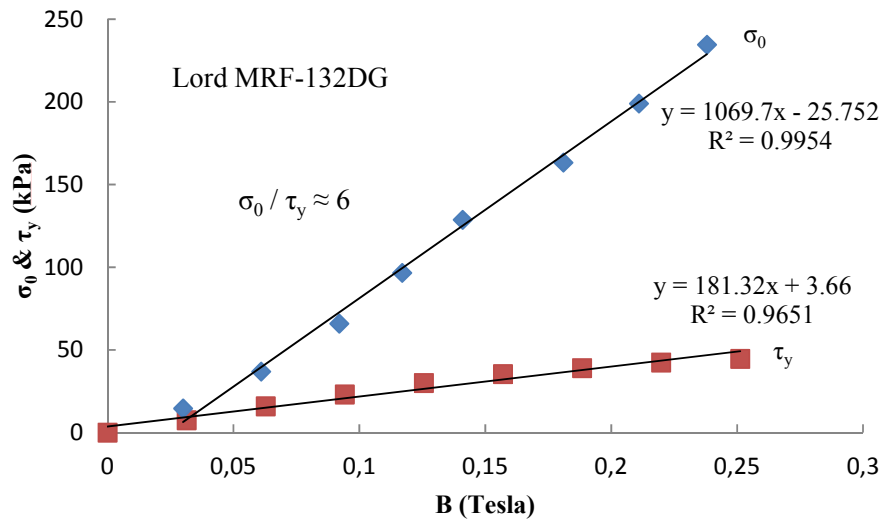
Figure 10. σ_o and τ_y vs. B (normalized to airgap).

Based on the observation that a translucent brown liquid with no evidence of particles (presumably the hydrocarbon oil host carrier fluid) appeared at the surface of the MR fluid during the compression, the authors propose the model shown in Fig.11 for the behavior in the present compression tests. In this model the host oil is squeezed out between the planar chain-like arrangement of the magnetic particles, thereby giving a slightly higher volume fraction of particles in the oil-depleted regions adjacent to and below the indenter. This in turn leads to an increase in stress required for further penetration of the indenter i.e. in the displacement, x. Due to the relative size difference between the indenter and sample container, in addition to the penetration depth, it is believed that interference from the walls or bottom of the container has a negligible effect on the experimental results.
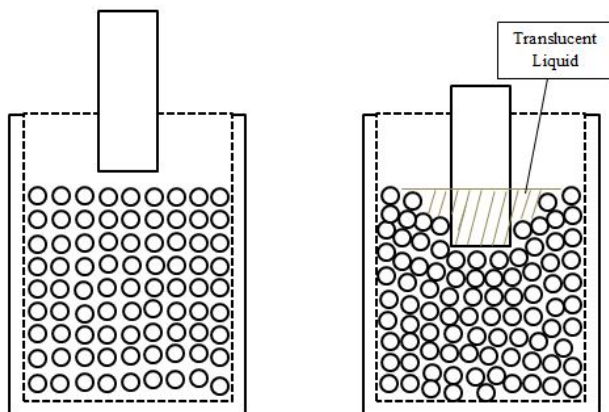

Figure 11. Model for the stress corresponding to the compression of the MRF. With penetration, the oil is squeezed out between the magnetic particles up along the side of the indenter, giving a higher volume fraction of particles below the indenter and in turn a higher stress with increasing penetration.

Accepting the above model, the decrease in stress which occurs when the field is turned on in the on-off tests can result from a disruption in the lower-energy, chain-like structure of the particles during the

displacement when the field is off. The more frequently this on-off transition occurs, the greater is the disruption and the lower the resistance to further displacement.

According to our model, the resistive tensile pull which acts on the indenter immediately following the reversal of the indenter could result from the presence of elastic compression strain in the chains below the bottom of the indenter and from the interaction between particles at the side surfaces of the indenter.

References
[1] Carlsen D 2005 MR Fluids and Devices in a Real World *Electrorheological Fluids and Magnetorheological Suspensions* K. Lu, R. Shen and J. Lu, eds., World Scientific, Singapore pp 531
[2] Goncalves F D and Carlson J D 2007 Investigating the time dependence of the MR effect *Int. J. Mod. Phys. B* **21** 4832
[3] Tang X, Chen Y and Conrad H 1996 Structure and interaction force in a model magnetorheological system J. *Intel. Mater. Syst. Struct.* **7** 517
[4] Ginder J M and Davis L C 1994 Shear stresses in magnetorheological fluids, Role of magnetic saturation *Appl. Phys. Lett.* **65** 3410
[5] Tang X and Conrad H 1996 Quasistatic measurements on a magnetorheological fluid *J. Rheol.* **40** 1167